Katholieke Universiteit Leuven

Departement Elektrotechniek

ESAT-SISTA/TR 10-239

A Low-Complexity Robust Capon Beamformer for Small Arrays[1]

Kim Ngo[2], Marc Moonen[2],
Douglas L. Jones [3]

November 2010
Submitted for publication in IEEE signal processing

[1]This report is available by anonymous ftp from *ftp.esat.kuleuven.be* in the directory *pub/sista/kngo/reports/10-239.pdf*

[2]K.U.Leuven, Dept. of Electrical Engineering (ESAT), Research group SCD (SISTA) Kasteelpark Arenberg 10, 3001 Leuven, Belgium, Tel. +32 16 321797, Fax +32 16 321970, WWW: *http://homes.esat.kuleuven.be/~kngo*. E-mail: *kim.ngo@esat.kuleuven.be*. This research work was carried out at the University of Illinois and at the ESAT Laboratory of Katholieke Universiteit Leuven, in the frame of K.U. Leuven Research Council CoE EF/05/006 Optimization in Engineering (OPTEC), Concerted Research Action GOA-MaNet, the Belgian Programme on Interuniversity Attraction Poles initiated by the Belgian Federal Science Policy Office IUAP P6/04 (DYSCO, 'Dynamical systems, control and optimization', 2007-2011), Research Project FWO nr. G.0600.08 ('Signal processing and network design for wireless acoustic sensor networks'), IWT Project 'Signal processing and automatic fitting for next generation cochlear implants' and EC-FP6 project SIGNAL: 'Core Signal Processing Training Program'. The scientific responsibility is assumed by its authors.

[3]University of Illinois at Urbana-Champaign, Department of Electrical and Computer Engineering, 1406 W. Green St., Urbana, Illinois 61801, USA, E-mail: dl-jones@illinois.edu

Abstract

The standard Capon beamformer (SCB) suffers from a substantial performance degradation when there is a mismatch between the presumed and the actual steering vector of the target signal. This has motivated the development of many robust Capon beamformer (RCB) techniques. However, these are mostly based on optimization procedures that are very computationally expensive. We present a new, low complexity RCB based on gradient maximization of the beamformer output where the steering vector is estimated within a predefined uncertainty region around the presumed steering vector. The proposed RCB offers a low complexity, simple implementation and no loss of degrees of freedom for interference suppression which is of great importance when dealing with small arrays. Experimental results with two omnidirectional microphones demonstrate that the proposed RCB outperforms the SCB in terms of output SNR and signal distortion. Simulations performed for scenarios with two or more competing speakers in a reverberant room show a 7dB gain in SNR and up to 3dB less signal distortion.

A Low-Complexity Robust Capon Beamformer for Small Arrays

Kim Ngo*, *Student Member, IEEE*, Douglas L. Jones, *Fellow, IEEE*, and Marc Moonen, *Fellow, IEEE*

Abstract

The standard Capon beamformer (SCB) suffers from a substantial performance degradation when there is a mismatch between the presumed and the actual steering vector of the target signal. This has motivated the development of many robust Capon beamformer (RCB) techniques. However, these are mostly based on optimization procedures that are very computationally expensive. We present a new, low complexity RCB based on gradient maximization of the beamformer output where the steering vector is estimated within a predefined uncertainty region around the presumed steering vector. The proposed RCB offers a low complexity, simple implementation and no loss of degrees of freedom for interference suppression which is of great importance when dealing with small arrays. Experimental results with two omnidirectional microphones demonstrate that the proposed RCB outperforms the SCB in terms of output SNR and signal distortion. Simulations performed for scenarios with two or more competing speakers in a reverberant room show a 7dB gain in SNR and up to 3dB less signal distortion.

Index Terms

Robust Capon beamformer, MVDR, steering vector uncertainty, non-stationary sources, hearing aids.

This research work was carried out at the University of Illinois and at the ESAT Laboratory of Katholieke Universiteit Leuven, in the frame of K.U. Leuven Research Council CoE EF/05/006 Optimization in Engineering (OPTEC), Concerted Research Action GOA-MaNet, the Belgian Programme on Interuniversity Attraction Poles initiated by the Belgian Federal Science Policy Office IUAP P6/04 (DYSCO, 'Dynamical systems, control and optimization', 2007-2011), Research Project FWO nr. G.0600.08 ('Signal processing and network design for wireless acoustic sensor networks'), IWT Project 'Signal processing and automatic fitting for next generation cochlear implants' and EC-FP6 project SIGNAL: 'Core Signal Processing Training Program'. The scientific responsibility is assumed by its authors.

K. Ngo and M. Moonen are with the Department of Electrical Engineering, Katholieke Universiteit Leuven, ESAT-SCD, Kasteelpark Arenberg 10, B-3001 Leuven, Belgium, (e-mails: {kim.ngo,marc.moonen}@esat.kuleuven.be).

D. L. Jones is with the Department of Electrical and Computer Engineering, University of Illinois at Urbana-Champaign, 1406 W. Green St., Urbana, Illinois 61801, USA, (e-mail: dl-jones@illinois.edu).

I. INTRODUCTION

Beamforming is used in many areas, such as radar, sonar, wireless communication, speech communication, and hearing aids. Hearing aids are a special case that imposes several constraints on a typical beamformer design. First of all, the size of a hearing aid is small hence only a small number of microphones can be used and furthermore these microphones will be spaced very close to each other. Secondly, beamformers for hearing aids should be designed to be robust against the case where multiple competing speakers are present, which is referred to as a cocktail-party scenario, i.e., the case where the number of interferes exceeds the number of microphones. Thirdly, suppression of interfering speech sources requires fast and accurate tracking, since speech signals are highly non-stationary and the speakers may change position with respect to the listener over time. Finally, the beamformer should also be robust against room reverberation, microphone mismatch, correlation between sources, mismatch between the presumed and the actual steering vector of the target signal.

In general, beamformers can be classified as either fixed beamformers or adaptive beamformers. In fixed beamforming, the filter coefficients are fixed for a predefined target signal position and are hence data-independent. The success of fixed beamformers relies on correct assumptions on the microphone characteristics, array geometry, target signal position etc. Well-known fixed beamformers are filter-and-sum beamformers and delay-and-sum beamformers [1][2]. Adaptive beamformers make use of data-dependent filter coefficients that are adapted to non-stationary signals and environments. The data-dependent beamformer proposed by Capon [3], referred to here as the standard Capon Beamformer (SCB) and also known as the minimum variance distortionless response (MVDR) beamformer, is a widely-used adaptive beamformer technique. The signal-to-noise ratio (SNR) performance of the SCB is often much better compared to the data-independent beamformers, particularly for small arrays. The SCB works well when the steering vector of the target signal is known precisely and a satisfactorily large number of snapshots are available for estimating the required correlation matrices. However, in most practical situations there is a mismatch between the presumed and the actual steering vector of the target signal.

Many approaches have been proposed to improve the robustness of the SCB. A variation of the SCB is known as the linearly constrained minimum variance (LCMV) beamformer [4] where a set of linear constraints is added. These constraints broaden the main beam by imposing a set of unity-gain constraints for steering vectors close to the presumed steering vector of the target signal such that robustness against a steering vector mismatch is achieved. A drawback with the LCMV is that each constraint removes one degree of freedom for interference suppression. Other robust extensions of the SCB have been based on diagonal loading of the sample correlation matrix [5][6]. The main problem with these approaches is to find the optimal value of the diagonal loading factor and that it reduces performance and the beam sharpness. Recent approaches estimate the diagonal loading factor based on the uncertainty region of the

presumed steering vector of the target signal. These methods are robust against target signal suppression when the actual steering vector is within the predefined uncertainty region. Spherical [7][8], ellipsoid [9][10][11][12][13] and polyhedron [14] uncertainty regions have all been studied.

In [15][16] it is shown that a frequency-domain SCB outperforms a time-domain Frost beamformer and a generalized sidelobe canceler for a scenario with two or more nonstationary interfering speech sources and an array with two microphones. A frequency-domain SCB exploits the time-frequency sparseness of the sources better than a time-domain implementation. The work in [15][16] uses a fixed steering vector for the target signal; the goal in this paper is to extend the frequency-domain SCB to an adaptive frequency-domain RCB. The RCB proposed here is based on a gradient approach where the steering vector is estimated based on a predefined level of uncertainty in the steering vector. The proposed RCB offers a low complexity, simple implementation and suffers no loss of degrees of freedom for interference suppression.

The paper is organized as follows. Section II defines the notation and reviews the SCB. Section III reviews the previous work on RCB. Section IV explains the ideas behind the proposed RCB. In Section V experimental results are presented. The work is summarized in Section VI.

II. Background

A. Notation and definitions

For an M-microphone system, the time-frequency-domain signals $X_i(k,l), i = 1, ..., M$ are represented as

$$X_i(k,l) = X_i^s(k,l) + X_i^n(k,l) \tag{1}$$

where k is the frequency bin index and l the frame index of a short-time Fourier transform, and the superscripts s and n are used to refer to the target signal, and the interference-plus-noise components, respectively. Let $\mathbf{X}(k,l) \in \mathbb{C}^{M\times 1}$ be defined as the stacked vector

$$\mathbf{X}(k,l) = [X_1(k,l)\ X_2(k,l)\ ...\ X_M(k,l)]^T = \mathbf{X}^s(k,l) + \mathbf{X}^n(k,l) \tag{2}$$

where the superscript T denotes the transpose. In addition, the correlation matrix can be recursively updated for each frequency bin as

$$\mathbf{R}(k,l+1) = \lambda\mathbf{R}(k,l) + (1-\lambda)\mathbf{X}(k,l+1)\mathbf{X}^H(k,l+1) \tag{3}$$

where H denotes Hermitian transpose λ is the forgetting factor. The output $Z(k,l)$ of a beamformer can be written as

$$Z(k,l) = \mathbf{W}^H(k,l)\mathbf{X}(k,l). \tag{4}$$

where $\mathbf{W}(k,l) = [W_1(k,l)\ ...\ W_M(k,l)]^T \in \mathbb{C}^{M\times 1}$ is the complex vector of beamformer weights.

The frequency bin index k and frame index l are omitted in the sequel for the sake of conciseness.

B. Standard Capon Beamformer

The goal of the SCB is to minimize the total beamformer output variance while constraining the target signal response to be unity to prevent target signal suppression. The SCB design can be formulated as

$$\min_{\mathbf{W}} \mathbf{W}^H \mathbf{R} \mathbf{W}, \quad \text{s. t.} \quad \bar{\mathbf{e}}^H \mathbf{W} = 1 \tag{5}$$

where $\min$ represents the minimization of a function with respect to the selected variables (the weights, $\mathbf{W}$, in this case), and $\bar{\mathbf{e}}$ is the presumed steering vector of the target signal. The closed-form solution to (5) is given by Capon [3] as

$$\mathbf{W} = \frac{\mathbf{R}^{-1}\bar{\mathbf{e}}}{\bar{\mathbf{e}}^H \mathbf{R}^{-1} \bar{\mathbf{e}}}, \tag{6}$$

where the output power σ^2 is given by

$$\sigma^2 = \frac{1}{\bar{\mathbf{e}}^H \mathbf{R}^{-1} \bar{\mathbf{e}}}. \tag{7}$$

C. Mismatch between presumed and actual steering vector

As mentioned, the SCB does not provide robustness against the case where there is a mismatch between the presumed and the actual steering vectors $\bar{\mathbf{e}}$ and $\mathbf{e}_{\text{x}}$, respectively. The mismatch between the presumed and the actual steering vector can be described as

$$\boxed{\mathbf{e}_{\text{x}} = \bar{\mathbf{e}} + \Delta_{\bar{\mathbf{e}}}} \tag{8}$$

where $\Delta_{\bar{\mathbf{e}}}$ is an unknown complex vector. Under such mismatch the constraint $\bar{\mathbf{e}}^H \mathbf{W}$=1 leads to part of the target signal being suppressed and hence a degradation in SNR and signal distortion. The goal is then to design a RCB that can compensate for the mismatch $\Delta_{\bar{\mathbf{e}}}$ by estimating the actual steering vector $\mathbf{e}_{\text{x}}$.

III. Previous work on Robust Capon Beamformers

In the past, many RCB approaches have been proposed. In this section, we briefly review some popular methods such as the LCMV beamformer, the diagonal-loading-based beamformer, and the uncertainty-based beamformer.

A. LCMV beamformer

In [4][17] the LCMV beamformer is proposed where the linear constraint in (5) is generalized such that the output power is minimized while restricting the filter weights to satisfy one or more linear equality constraints. The LCMV design can be formulated as

$$\min_{\mathbf{W}} \mathbf{W}^H \mathbf{R} \mathbf{W}, \quad \text{s. t.} \quad \mathbf{C}^H \mathbf{W} = \mathbf{f} \tag{9}$$

where $\mathbf{C}$ is the constraint matrix and the vector $\mathbf{f}$ specifies the corresponding constraint value for each vector. These additional linear constraints can be either directional constraints [18] or derivative constraints [19][20], where the core idea is to broaden the main beam of the beampattern so that it is more robust against steering vector mismatch. It should however be mentioned that for every additional linear constraint imposed, the beamformer loses one degree of freedom for interference suppression, which is undesirable for small arrays.

B. Diagonal-loading-based beamformer

In the diagonal-loading-based RCB is proposed where a regularization of the correlation matrix is included. The diagonal-loading-based RCB design can be formulated as

$$\min_{\mathbf{W}} \mathbf{W}^H(\mathbf{R}+\gamma\mathbf{I})\mathbf{W}, \quad \text{s. t.} \quad \bar{\mathbf{e}}^H\mathbf{W}=1 \tag{10}$$

where γ is the regularization factor and $\mathbf{I}$ is the identity matrix. The problem here is the difficulty of specifying the optimal value of γ. If γ is set too large the beamformer loses interference suppression performance, and if γ is set too small the robustness is sacrificed.

C. Uncertainty-based beamformer

A recent robust beamforming approach suggests that the steering vector mismatch can be accounted for based on a predefined uncertainty region around the presumed steering vector. The uncertainty-based RCB design can be formulated as [13]

$$\min_{\mathbf{W}} \mathbf{W}^H\mathbf{R}\mathbf{W}, \quad \text{s. t.} \quad |\mathbf{W}^H(\bar{\mathbf{e}}+\Delta)| \geq 1, \quad \text{for all} \quad \|\Delta\| \leq \varepsilon \tag{11}$$

where Δ is the steering vector mismatch as in (8) and ε denotes the uncertainty region. This contraint forces the magnitude responses for an uncertainty set of steering vectors to exceed unity. The drawback of the uncertainty-based RCB formulation in (11) is the infinite number of constraints. The performance is said to be optimal if ε is large enough to cover the mismatch between the presumed and the actual steering vector of the target signal. In [7] the problem is reformulated as a second-order cone programming problem, based on a spherical uncertainty set, which can be solved (although at very high computational complexity) using the well-established interior-point method. In order to use standard optimization techniques, the uncertainty region has often been generalized to an ellipsoid [9][10][11] or a polyhedron [14].

D. Max-min optimization

An alternative consists in estimating the steering vector $\mathbf{e}$ which results in the maximal output power [6][21], i.e.,

$$\boxed{\max_{\mathbf{e}} \min_{\mathbf{W}} \mathbf{W}^H\mathbf{R}\mathbf{W}, \quad \text{s. t.} \quad \mathbf{e}^H\mathbf{W}=1, \|\mathbf{e}\|^2=1} \tag{12}$$

where the unit norm is included to avoid a scaling ambiguity in the output power. With (7) the expression in (12) can be simplified to

$$\max_{\mathbf{e}} \frac{1}{\mathbf{e}^H\mathbf{R}^{-1}\mathbf{e}} = \min_{\mathbf{e}} \mathbf{e}^H\mathbf{R}^{-1}\mathbf{e}, \quad \text{s. t.} \quad \|\mathbf{e}\|^2 = 1, \tag{13}$$

This is a principal eigenvector problem where the eigenvalue corresponding to the largest eigenvalue of $\mathbf{R}$ provides the optimal steering vector $\mathbf{e}$. If the target signal is not the dominant signal the solution in (13) leads to a wrong solution. In this case a subset of eigenvalues (signal plus interference) can be chosen at the cost of a reduced resolution [21]. The problem in (13) has been reformulated in [10] as

$$\boxed{\min_{\mathbf{e}} \mathbf{e}^H\mathbf{R}^{-1}\mathbf{e} \quad \text{s. t.} \quad \|\mathbf{e}-\bar{\mathbf{e}}\|^2 \leq \varepsilon.} \tag{14}$$

The idea behind (14) is illustrated in Fig. 1. The radius ε of the sphere defines the uncertainty region, and the goal is then to design the beamformer to maximize the SNR over the whole uncertainty region. The challenge is then to find an optimal value for the radius ε. If ε is set too large the beamformer loses degrees of freedom for interference suppression, if ε is set too small the uncertainty region may not be sufficient to compensate for the steering vector mismatch. It is also clear that, when the sphere reduces to a single point, the method is equivalent to the SCB.

IV. Proposed Robust Capon Beamformer

Previous practical RCB methods mostly belong to the class of diagonal-loading-based beamformers [7][9][10][11], where the amount of diagonal loading is calculated based on the uncertainty region around the presumed steering vector. This form of regularization reduces the beamformer's interference suppression capabilities, particularly for small arrays. In this section, we present a RCB that exploits the same uncertainty region but does not depend on a diagonal loading. The new method can obtain both robustness and much greater interference suppression with small arrays.

A. Proposed RCB formulation

The problem is that we obviously do not know the exact steering vector, only a region in which it should lie, i.e., if the selected vector from this region differs from the actual steering vector, the beamformer will attempt to minimize the output power by suppressing the signal plus interference. If the selected vector is equal to the actual steering vector, the beamformer cannot cancel the signal which leads to a larger output power. The proposed RCB formulation, when the uncertainty region is defined as a sphere, can be written as

$$\boxed{\max_{\mathbf{e}} \min_{\mathbf{W}} \mathbf{W}^H\mathbf{R}\mathbf{W}, \quad \text{s. t.} \quad \mathbf{e}^H\mathbf{W} = 1, \|\mathbf{e}-\bar{\mathbf{e}}\|^2 \leq \varepsilon, \|\mathbf{e}\|^2 = \|\bar{\mathbf{e}}\|^2} \tag{15}$$

The proposed RCB differs from (11) in that instead of insisting that $|\mathbf{W}^H(\bar{\mathbf{e}}+\Delta)| \geq 1$ for the entire uncertainty region; an optimal steering vector is now estimated within the uncertainty region such that

$\mathbf{e}^H\mathbf{W}$=1 for that particular distortionless response and hence the beamformer can do whatever is best elsewhere in the uncertainty region, thus allowing better performance in terms of suppressing interference. So, instead of having multiple constraints we now have a single adapted constraint. The proposed RCB also differs from (14) in that an additional constraint is included to avoid a scaling ambiguity (as in (12)), since the uncertainty region is defined as a sphere and certain steering vectors can therefore increase the power. The constraint $\|\mathbf{e}\|^2$=$\|\bar{\mathbf{e}}\|^2$ therefore ensures that the estimated steering vector has the same power as the presumed steering vector.

The proposed RCB is shown in Fig. 2 such that the estimated steering vector lies within the uncertainty region, i.e., the beamformer is allowed to steer in certain directions as long as it remains within the predefined uncertainty region. Increasing or decreasing ε in our case only impacts the steering capabilities. The proposed RCB therefore suffers no loss of degrees of freedom for interference suppression, since the width of the beam is not increased. The proposed RCB also has the advantage of a low complexity and simple implementation, since the solution does not include an infinite number of constraints and hence a closed-form update expression can be derived.

Using the output power defined in (7), the optimization problem can be written as

$$\boxed{\min_{\mathbf{e}} \mathbf{e}^H\mathbf{R}^{-1}\mathbf{e}, \quad \text{s. t.} \quad \|\mathbf{e}-\bar{\mathbf{e}}\|^2 \leq \varepsilon, \|\mathbf{e}\|^2 = \|\bar{\mathbf{e}}\|^2.} \tag{16}$$

As with all robust beamformers based on an uncertainty region, success depends on selecting a proper value of ε, since a large ε value may cause the steering vector to steer towards the interferences and a small ε value may not be sufficient to accommodate the steering vector mistmatch.

B. Gradient update of the steering vector

The gradient of the output power with respect to the estimated steering vector $\mathbf{e}$ can be estimated as:

$$\nabla\mathbf{e} = \frac{d}{d\mathbf{e}}\left(\mathbf{e}^H\mathbf{R}^{-1}\mathbf{e}\right) = -2\mathbf{R}^{-1}\mathbf{e}. \tag{17}$$

Additionally, we propose to project the gradient onto the tangent plane:

$$\hat{\nabla}\mathbf{e} = \nabla\mathbf{e} - \mathbf{e}\frac{\mathbf{e}^H\nabla\mathbf{e}}{\|\mathbf{e}\|^2}. \tag{18}$$

The projection of the gradient onto the tangent plane is shown in Fig. 3. Assuming that the gradient change is small, the benefit of the projection is that it remains close to the constrained steering vector norm, i.e., $\|\mathbf{e}\|^2$=$\|\bar{\mathbf{e}}\|^2$. Furthermore, projecting the gradient onto the tangent plane before estimating the stepsize guarantees that any step remains within the tangent plane, which may not be the case if the projection is performed after the estimation of the stepsize. The stepsize in the gradient direction (tangent plane) can be calculated as follows:

$$\min_{\mu}(\mathbf{e}+\mu\hat{\nabla}\mathbf{e})^H\mathbf{R}^{-1}(\mathbf{e}+\mu\hat{\nabla}\mathbf{e}), \quad \text{s. t.} \quad \|\mu\hat{\nabla}\mathbf{e}\|^2 \leq \|\alpha\mathbf{e}\|^2 \tag{19}$$

where α controls the maximum stepsize change for each update. The constraint limits the change in the steering vector so as to avoid potential adaptation noise or artifacts. The maximum stepsize yields a maximum reduction in the error criterion at each update. The stepsize μ can be found by differentiating (19) with respect to μ:

$$\frac{d}{d\mu}(\mathbf{e}+\mu\hat{\nabla}\mathbf{e})^H\mathbf{R}^{-1}(\mathbf{e}+\mu\hat{\nabla}\mathbf{e}) \tag{20}$$

and setting the derivative to zero

$$\hat{\nabla}\mathbf{e}^H\mathbf{R}^{-1}\mathbf{e}+\mathbf{e}^H\mathbf{R}^{-1}\hat{\nabla}\mathbf{e}+2\mu\hat{\nabla}\mathbf{e}^H\mathbf{R}^{-1}\hat{\nabla}\mathbf{e}=0 \tag{21}$$

gives

$$\mu=-\frac{\hat{\nabla}\mathbf{e}^H\mathbf{R}^{-1}\mathbf{e}+\mathbf{e}^H\mathbf{R}^{-1}\hat{\nabla}\mathbf{e}}{2\hat{\nabla}\mathbf{e}^H\mathbf{R}^{-1}\hat{\nabla}\mathbf{e}}. \tag{22}$$

The estimated stepsize μ is only used if $\|\mu\hat{\nabla}\mathbf{e}\|^2 \leq \|\alpha\mathbf{e}\|^2$ otherwise the stepsize is normalized as

$$\mu=\alpha\frac{\|\mathbf{e}\|}{\|\hat{\nabla}\mathbf{e}\|}. \tag{23}$$

The steering vector is then updated as follows:

$$\hat{\mathbf{e}}=\mathbf{e}+\mu\hat{\nabla}\mathbf{e}, \tag{24}$$

and is selected if $\|\hat{\mathbf{e}}-\bar{\mathbf{e}}\|^2 \leq \varepsilon$ otherwise the previous estimated steering vector is selected. To satisfy the norm constrant in (16) the normalized updated steering vector can be written as

$$\hat{\mathbf{e}}=\hat{\mathbf{e}}\frac{\|\bar{\mathbf{e}}\|}{\|\hat{\mathbf{e}}\|}. \tag{25}$$

C. Computational complexity

The computational complexity of the SCB is analysed in [15] and here we will analyse the complexity of the proposed RCB. The comparison is made in terms of real additions, real multiplications, and real divisions, by assuming that two real additions are required for each complex addition, four real multiplications and two real additions are required for each complex multiplication, and two complex multiplications and two real divisions for each complex division are required. Table I summarizes the computational complexity, for an example with M=2 (number of microphones) and K=64 (FFT length).

V. Experimental Results

A. Experimental set-up

Simulations have been performed in a reverberant rectangular conference room with dimensions 9m x 4m x 2.75m (length x width x height) and a reverberation time, T_{60}=0.37s, with two omnidirectional

Part of RCB algorithm	Complex additions	Complex multiplies	Real additions	Real multiplies	Real divisions
Gradient estimation	0	0	0	0	0
Projection	$M+(M-1)\left(\frac{K}{2}+1\right)$	$2M\left(\frac{K}{2}+1\right)$	0	0	2
Stepsize	$M(M-1)\left(\frac{K}{2}+1\right)$	$M^2\left(\frac{K}{2}+1\right)$	$2M\left(\frac{K}{2}+1\right)$	$4M\left(\frac{K}{2}+1\right)$	$\left(\frac{K}{2}+1\right)$
Gradient update	$M\left(\frac{K}{2}+1\right)$	0	0	$2M\left(\frac{K}{2}+1\right)$	0
Stepsize constraint	0	0	$3M-1\left(\frac{K}{2}+1\right)$	$4M+2\left(\frac{K}{2}+1\right)$	$\left(\frac{K}{2}+1\right)$
Steering vector constraint	$2M\left(\frac{K}{2}+1\right)$	0	$2M-1\left(\frac{K}{2}+1\right)$	$2M+1\left(\frac{K}{2}+1\right)$	0
SCB [15]	-	-	2747	3007	66
Proposed RCB	-	-	4013	4570	70

TABLE I

TOTAL COMPUTATIONAL COMPLEXITY FOR THE PROPOSED RCB COMPARED TO SCB.

microphones in free-field separated by 15cm. Further details can be found in [15]. The loudspeakers are positioned at 1m from the microphones in the frontal horizontal plane at angles ranging from -90° to +90° relative to the microphones, with a spacing of 15°, which is illustrated in Fig. 4.

The speech signals consist of male and female sentences each approximately 2.5s. in duration. The signals are sampled at 22.05 kHz. The spatial scenarios used in the simulations are listed in Table 5. A total of three simulations are performed, i.e., the case with two, three and four interferences. For each simulation the first 2.5s sentence uses the configuration "a" and the next 2.5s sentence uses the configuration "b". The beamformer is evaluated for a different range of input SNR's and for different values of λ defined in (3). An FFT length of 1024 with 50% overlap was used in all simulations. The radius ε of the uncertainty region is defined as ε=$||\beta\bar{\mathbf{e}}||^2$.

B. Performance measures

To assess the noise reduction performance the intelligibility-weighted SNR is used which is defined as

$$\Delta\text{SNR}_{\text{intellig}} = \sum_i I_i(\text{SNR}_{i,out} - \text{SNR}_{i,in}) \tag{26}$$

where I_i is the band importance function [22] and where $\text{SNR}_{i,out}$ and $\text{SNR}_{i,in}$ represent the output SNR and the input SNR (in dB) of the *i*-th band, respectively. For measuring the signal distortion a frequency-weighted log-spectral signal distortion (SD) is used, defined as

$$\text{SD} = \frac{1}{K}\sum_{k=1}^{K}\sqrt{\int_{f_l}^{f_u} w_{ERB}(f)\Big(10log_{10}\frac{P^s_{out,k}(f)}{P^s_{in,k}(f)}\Big)^2 df} \tag{27}$$

where K is the number of frames, $P^s_{out,k}(f)$ is the output power spectrum of the kth frame, $P^s_{in,k}(f)$ is the input power spectrum of kth frame, and f is the frequency index. The SD measure is calculated with a frequency-weighting factor $w_{ERB}(f)$ giving equal weight for each auditory critical band.

C. Results

The SNR and SD for the three cases are shown in Fig. 6, 7 and 8. The performance benefits in terms of output SNR of the proposed RCB is clear, especially when λ =0.3 and λ=0.6 with β=0.35, and furthermore the distortion is also much lower. When λ=0.9 the performance of the proposed RCB is closer to the SCB (especially at low input SNR) but the benefit still remains at higher input SNR. It is worth noting that the case with two interferes the SCB outperforms the RCB with β=0.35 at low input SNR, but this can be avoided when β=0.15. This does not seem to happen for the case with three and four interferes, which suggest that for the case with two interferes, λ=0.9 was sufficient to track the non-stationarity of the sources. It is clear that the performance of the SCB highly depends on the accuracy of the estimated correlation matrices, whereas the proposed RCB is more robust. The reduced performance when λ=0.9 for the proposed RCB can be caused by the limited tracking performance.

VI. Conclusion

In this paper, a frequency-domain RCB is presented which is based on a gradient approach where the steering vector is estimated based on a predefined uncertainty region of the steering vector mismatch. Experimental results for a scenario with a microphone array containing two omnidirectional microphones and with competing speakers in a reverberant room demonstrate that the proposed RCB outperforms the SCB in terms of output SNR and signal distortion. The proposed RCB showed robustness especially in the case where a small forgetting factor was used to estimate the correlation matrices, whereas the SCB showed a significant performance degradation. Furthermore, the proposed RCB offers a low complexity, simple implementation and no loss of degrees of freedom for interference suppression.

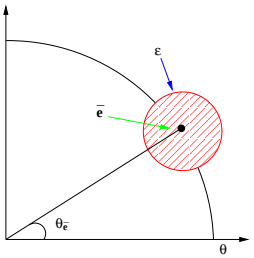


Fig. 1. Hyperplane for the RCB defined in (14).

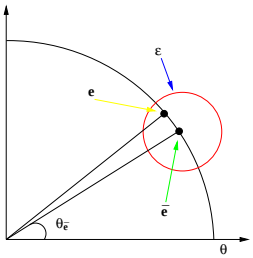


Fig. 2. Hyperplane for the proposed RCB defined in (16).

References

[1] S. Doclo and M. Moonen, "Design of broadband beamformers robust against gain and phase errors in the microphone array characteristics," *IEEE Trans. Signal Processing*, vol. 51, no. 10, pp. 2511–2526, Oct. 2003.

[2] B. D. Van Veen and K. M. Buckley, "Beamforming: A versatile approach to spatial filtering," *IEEE ASSP Magazine*, vol. 5, no. 2, pp. 4–24, Apr. 1988.

[3] J. Capon, "High-resolution frequency-wavenumber spectrum analysis," *Proc. IEEE*, vol. 57, no. 8, pp. 1408–1418, Aug. 1969.

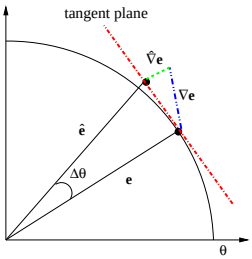


Fig. 3. Gradient projected onto the tangent plane.

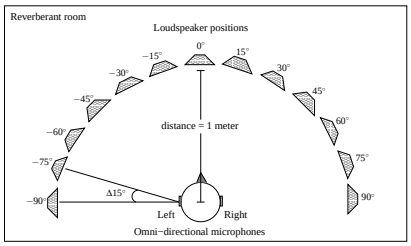


Fig. 4. Simulation setup with loudspeaker positions.

Case	Azimuth angle of source
1a	Target at 0°, single-talker at -30° and 30°
1b	Target at 0°, single-talker at -45° and 45°
2a	Target at 0°, single-talker at -90°, -30° and 45°
2b	Target at 0°, single-talker at -90°, 45° and 75°
3a	Target at 0°, single-talker at -90°, -45°, 45° and 90°
3b	Target at 0°, single-talker at -90°, -30°, 30° and 90°

Fig. 5. Spatial scenarios

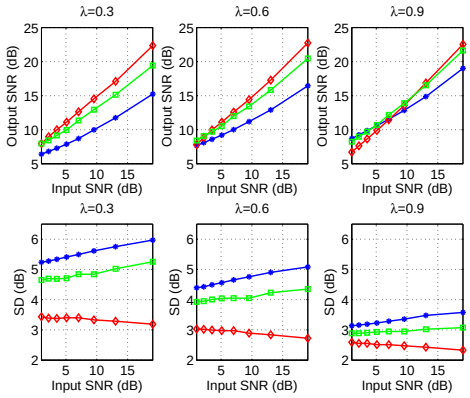


Fig. 6. SNR and SD for two interferes for different values of λ and α. (*) SCB, (□) RCB ($\beta = 0.15$), (◊) RCB ($\beta = 0.35$).

[4] O. L. Frost, III, "An algorithm for linearly constrained adaptive processing," *Proc. IEEE*, vol. 60, pp. 926–935, Aug. 1972.

[5] C.-Y. Chen and P. Vaidyanathan, "Quadratically constrained beamforming robust against direction-of-arrival mismatch," *IEEE Trans. Signal Processing*, vol. 55, no. 8, pp. 4139–4150, aug. 2007.

[6] Z. L. Yu and M. H. Er, "A Robust Capon Beamformer against Uncertainty of Nominal Steering Vector," *EURASIP Journal on Applied Signal Processing*, vol. Article ID 62327, pp. 1–8, 2006, doi:10.1155/ASP/2006/62327.

[7] S. A. Vorobyov, A. B. Gershman, and Z.-Q. Luo, "Robust Adaptive Beamforming Using Worst-Case Performance

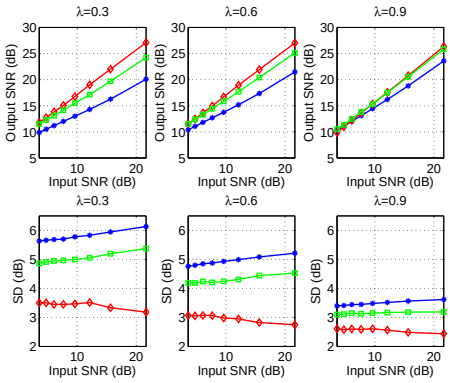


Fig. 7. SNR and SD for three interferes for different values of λ and α. (*) SCB, (□) RCB ($\beta = 0.15$), (◊) RCB ($\beta = 0.35$).

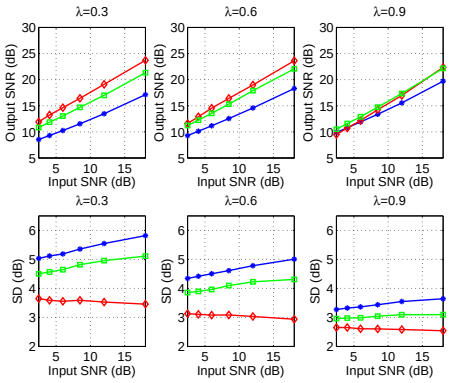


Fig. 8. SNR and SD for four interferes for different values of λ and α. (*) SCB, (□) RCB ($\beta = 0.15$), (◊) RCB ($\beta = 0.35$).

Optimization: A Solution to the Signal Mismatch Problem," *IEEE Trans. Signal Processing*, vol. 51, no. 2, pp. 312–324, Feb. 2003.

[8] J. Li, P. Stoica, and Z. Wang, "Doubly Constrained Robust Capon Beamformer," *IEEE Trans. Signal Processing*, vol. 52, no. 9, pp. 2407–2423, 2004.

[9] R. G. Lorenz and S. P. Boyd, "Robust Minimum Variance Beamforming," *IEEE Trans. Signal Processing*, vol. 53, no. 5, pp. 1684–1696, May 2005.

[10] J. Li, P. Stoica, and Z. Wang, "On Robust Capon Beamforming and Diagonal Loading," *IEEE Trans. Signal Processing*, vol. 51, no. 7, pp. 1702–1715, 2003.

[11] A. Beck and Y. C. Eldar, "Doubly Constrained Robust Capon Beamformer With Ellipsoidal Uncertainty Sets," *IEEE Trans. Signal Processing*, vol. 55, no. 2, pp. 753–758, Feb. 2007.

[12] P. Stoica, Z. Wang, and J. Li, "Robust Capon Beamforming," *IEEE Trans. Signal Processing Letters*, vol. 10, no. 6, pp. 172–175, 2003.

[13] L. H. Lei, J. P. Lie, A. B. Gershman, and C. M. S. See, "Robust Adaptive Beamforming in Partly Calibrated Sparse Sensor Arrays," *IEEE Trans. Signal Processing*, vol. 58, no. 3, pp. 1661–1667, Mar. 2010.

[14] S. Q. Wu and J. Y. Zhang, "A new robust beamforming method with antennae calibration error," in *IEEE Wireless Commun. Networking Conf.*, New Orleans, USA, 1999, p. 869872.

[15] M. E. Lockwood, D. L. Jones, R. C. Bilger, C. R. Lansing, W. D. O'Brien, B. C. Wheeler, and A. S. Feng, "Performance of time- and frequency-domain binaural beamformers based on recorded signals from real rooms," *Acoustical Society of America Journal*, vol. 115, no. 1, pp. 379–391, Jan. 2004.

[16] M. E. Lockwood and D. L. Jones, "Beamformer performance with acoustic vector sensors in air," *Acoustical Society of America Journal*, vol. 119, no. 1, pp. 1–11, Jan. 2006.

[17] C. Y. Tseng and L. J. Griffiths, "A unified approach to the design of linear constraints in minimum variance adaptive beamformers," *IEEE Trans. Antennas Propag.*, vol. 40, no. 12, pp. 1533–1542, Dec. 1992.

[18] K. Takao, H. Fujita, and T. Nishi, "An adaptive antenna array under directional constraint," *IEEE Trans. Antennas Propag.*, vol. 24, no. 5, pp. 662–669, Sep. 1976.

[19] S. P. Applebaum and D. J. Chapman, "Adaptive arrays with main beam constraints," *IEEE Trans. Antennas Propag.*, vol. 24, no. 5, pp. 650–662, Sep. 1976.

[20] K. M. Buckley and L. J. Griffiths, "An adaptive generalized sidelobecanceler with derivative constraints," *IEEE Trans. Antennas Propag.*, vol. 34, no. 3, pp. 311–319, Mar. 1986.

[21] A. Pezeshki, B. Van Veen, L. Scharf, H. Cox, and M. Nordenvaad, "Eigenvalue beamforming using a multirank mvdr beamformer and subspace selection," *Signal Processing, IEEE Transactions on*, vol. 56, no. 5, pp. 1954 –1967, may. 2008.

[22] J. E. Greenberg, P. M. Peterson, and P. M. Zurek, "Intelligibility-weighted measures of speech-to-interference ratio and speech system performance," *J. Acoustic. Soc. Am.*, vol. 94, no. 5, pp. 3009–3010, Nov. 1993.